

Single-crystal Vibrational Spectrum of Benitoite, a Non-centrosymmetric Silicate Crystal, and some Comments on Beryl

By David M. Adams* and Ian R. Gardner, Department of Chemistry, The University, Leicester LE1 7RH

Benitoite, $\text{BaTiSi}_3\text{O}_9$, is a non-centrosymmetric crystal showing pronounced LO–TO splitting. An almost complete assignment was deduced from single-crystal i.r. reflectance and Raman data. For the E' species excellent agreement was found between i.r. and Raman observations, which were complementary. LO modes were observed directly in Raman back-scattering experiments. It is shown that the complex vibrational spectra of both benitoite and beryl are constructed from pairs of coupled ring frequencies (there are two silicate rings in each unit cell) together with Ti–O, Al–O, and Be–O stretches (as appropriate) at frequencies as high as 800 cm^{-1} .

BENITOITE, $\text{BaTiSi}_3\text{O}_9$, is a relatively rare mineral prized for its delicate blue colour. Its structure¹ bears a formal similarity to that of beryl, but in benitoite the rings consist of only three (SiO_4) tetrahedra and have symmetry C_{3h} . They pack in columns forming a unit cell with factor group symmetry D_{3h} , and herein lies a major part of the spectroscopic interest. The Raman spectra of crystals having non-centrosymmetric factor groups may show more bands than are predicted by group theory. The reason for this anomalous behaviour, first elucidated by Poulet,² is that when both i.r. and Raman activities are associated with the same symmetry species,

¹ R. W. G. Wyckoff, 'Crystal Structure,' Interscience, New York, 1948, vol. 4, p. 261.

² H. Poulet, *Compt. rend.*, 1952, **234**, 2185; 1954, **238**, 70.

the strong oscillating electric field of a vibrational mode can interact with scattered Raman phonons of the same symmetry, splitting them into longitudinal (LO) and transverse (TO) components, which may be observed separately with suitable choice of scattering geometry. In lattices with strongly directional bonding, such as hexagonal ZnO, the LO–TO splitting may be very large,³ and the relative scattering efficiencies are sometimes such that an LO mode is actually more intense than its TO component.⁴

Independent determination of LO and TO mode

³ T. C. Damen, S. P. S. Porto, and B. Tell, *Phys. Rev.*, 1966, **142**, 570.

⁴ P. F. Williams and S. P. S. Porto, *Phys. Rev. (B)*, 1973, **8**, 1782.

frequencies is also possible *via* i.r. reflectance from single-crystal faces at near normal incidence; the combination of this technique with the Raman measurements is powerful for any non-centrosymmetric crystal, but especially so for a complex crystal such as benitoite which has 40 optically active modes (not including degeneracies), and hence is likely to present cases of accidental degeneracy and weakness. Benitoite has not been studied previously by single-crystal techniques, although some i.r. and Raman frequencies have been listed for powder

shown⁸ that CaO and SrO are 91.3 and 92.6% ionic respectively. We may presume that the isostructural-(B1) BaO is even more ionic and non-directional in bond type and, hence, that the bonding between barium and its six nearest-neighbour oxygens in benitoite is also highly non-directional. Physically then, to speak of barium translational modes in benitoite is a good approximation. The T_{1u} phonon frequencies for CaO and SrO are 290 and 227 cm^{-1} respectively⁹ and that for BaO is estimated to be close to 190 cm^{-1} . Barium

TABLE I
Factor group analysis for $\text{BaTiSi}_3\text{O}_9$

D_{3h}	N_{total}	T_A	A				B				Si-O	Activities
			N_{opt}	T_{Ba}	R	N_{int}	N_{opt}	T	R	N_{int}		
A_1'	7		7	0	1	6	7	0	1	6	2	$xx + yy; zz$
A_2'	9		9	1	1	7	9	2	1	6	2	
E'	16	1	15	1	0	14	15	3	0	12	4	$(x, y); (xx - yy; xy)$
A_1''	5		5	0	0	5	5	1	0	4	1	z
A_2''	7	1	6	1	0	5	6	1	0	4	1	z
E''	12		12	1	2	9	12	2	2	8	2	$(yz; zx)$

N_{total} = total number of normal modes of primitive cell; T_A = acoustic modes; N_{opt} = optical branch modes; T = translatory modes, optic branch, of rings, Ba and Ti; R = rotatory modes of rings; N_{int} = modes of rings plus Ti; T_{Ba} = translatory modes of Ba^{2+} ; N_{int} = internal modes of rings; Si-O = representation spanned by the set of Si-O bond vectors.

samples.⁵ A further principal aim of this study was to establish the assignment and compare it with that recently made for beryl.⁶

Selection Rules.—Benitoite crystallises in the hexagonal system with the symmetry of space group D_{3h}^2 ($P\bar{6}c2$), $Z = 2$. The structure is illustrated in Figure 1, and the factor group analysis⁷ (f.g.a.) shown in Table 1. The optical branch modes, N_{opt} , may be further subdivided

translational modes in benitoite should therefore not be above 200 cm^{-1} .

The Ti-O bonds will be intermediate in type between the highly ionic Ba-O and the strongly covalent Si-O,

TABLE 2
Correlation scheme for the internal modes of the $\text{Si}_3\text{O}_9^{6-}$ rings in benitoite

Hypothetical ion, D_{3h}	Ion and site, C_{3h}	$\times 2$	Crystal, D_{3h}^2 †
$4a_1'$	$6A'$		$6(A_1' + A_2')$
$2a_2'$			
$6e'$	$6E'$		$12E$
a_1''	$4A''$		$4(A_1'' + A_2'')$
$3a_2''$			
$4e''$	$4E''$		$8E''$
$\nu(\text{Si-O})$ modes (b = bridging; t = terminal)			
Si-O _b $\left\{ \begin{array}{l} a_1' \\ e' \end{array} \right.$	A' E'		$A_1' + A_2'$ ‡ $2E'$
Si-O _t $\left\{ \begin{array}{l} a_1' \\ e' \\ a_2'' \\ e'' \end{array} \right.$	A' E' A'' E''		$A_1' + A_2'$ $2E'$ $A_1'' + A_2''$ $2E''$

† Identical with N_{int} of Table 1. ‡ Identical with Si-O of Table 1.

into sets originating as internal modes of the $\text{Si}_3\text{O}_9^{6-}$ rings, and various translatory and rotatory modes, but this is only a formalism unless there is a physical justification. Using a quantum-mechanically defined scale of ionicity in crystals of type AB, Phillips has recently

⁵ W. P. Griffith, *J. Chem. Soc. (A)*, 1967, 905.

⁶ D. M. Adams and I. R. Gardner, *J.C.S. Dalton*, 1974, 1502.

⁷ D. M. Adams and D. C. Newton, 'Tables for Factor Group and Point Group Analysis,' Beckman-RITC Limited, Croydon, 1970.

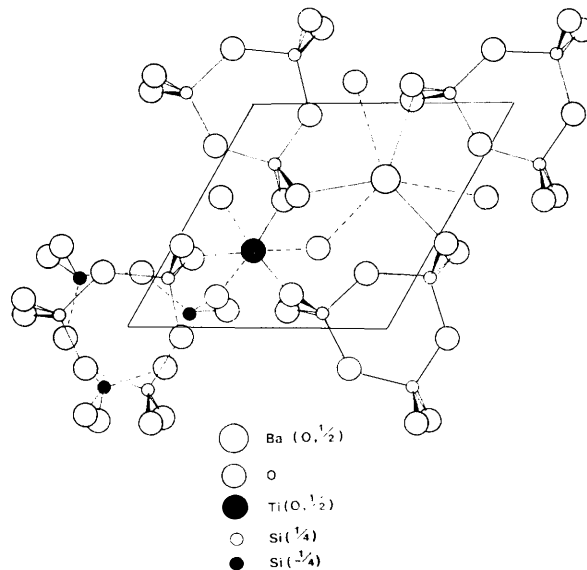


FIGURE 1 The crystal structure of benitoite, $\text{BaTiSi}_3\text{O}_9$

and probably comparable with those in rutile, a distinctly non-ionic lattice,¹⁰ with Raman phonon frequencies as high as 825 cm^{-1} .⁹ We therefore consider that the vibrational spectrum of benitoite is most realistically interpreted on the basis of the f.g.a. shown

⁸ J. C. Phillips, *Rev. Mod. Phys.*, 1970, 40, 373.

⁹ S. D. Ross, 'Inorganic Infrared and Raman Spectra,' McGraw-Hill, London, 1972.

¹⁰ D. M. Adams, 'Inorganic Solids,' Wiley, Chichester, 1974.

as Table 1A; on this view, the column N_{int} covers the internal modes of the rings plus the motions of Ti. The ring rotatory modes are given separately, although they are strictly also torsional modes of Ti-O bonds, to give an indication of the number of very low frequency bands; they were found by noting that the ring centres are on Wyckoff sites b . Table 1B shows how the mode descriptions are altered on the assumption that translational modes may be ascribed to both Ba^{2+} and Ti^{4+} .

LO-TO Splitting in the Raman spectra is confined to the E' species as this is the only one with both i.r. and Raman activities. The E' Raman tensor components interact with the macroscopic electric field components as shown below:¹¹

$$\begin{bmatrix} \cdot & d & \cdot \\ d & \cdot & \cdot \\ \cdot & \cdot & \cdot \end{bmatrix} \quad \begin{bmatrix} d & \cdot & \cdot \\ \cdot & d & \cdot \\ \cdot & \cdot & \cdot \end{bmatrix}$$

$E'(x)$ $E'(y)$

It follows that the components of E' generated in the scattering geometries used are as shown in Table 3. Note that in experiments $x(\rho\sigma)z$ the scattered phonon moves in a direction that is neither along the optic axis nor in a plane normal to it; accordingly it is not strictly correct to classify it either with a symmetry species or as of type LO or TO: such modes are indicated as $E(H)$ in Table 3. However, the above discussion of the bonding

TABLE 3

The scattering geometries used for benitoite and the mode types predicted

90° scatter:		180° scatter:	
$x(zz)y$	A_1'	$y(zz)\bar{y}$	A_1'
$x(yx)y$	$E'(LO + TO)$	$y(zx)\bar{y}$	E''
$x(zx)y$	E''	$y(xx)\bar{y}$	$A_1' + E'(LO)$
$x(yz)y$	E''	$z(xx)\bar{z}$	$A_1' + E'(TO)$
		$z(xy)\bar{z}$	$E'(TO)$
$x(yy)z$	$A_1' + E'(TO)$	$z(yy)\bar{z}$	$A_1' + E'(TO)$
$x(yx)z$	$E'(H)$		
$x(zx)z$	E''		
$x(yx)z$	E''		

in benitoite clearly implies that this is a crystal in which long-range electrostatic forces will be important and will predominate over any anisotropy in the force constants in determining the principal features of the lattice dynamics. In such cases departures from the simple mode classifications and descriptions are expected to be slight¹¹ and, in fact, none were detected by us.

A scheme of coupling of modes from the two rings in the cell is shown in Table 2: it implies that, unless the correlation field is very strong, the resultant modes should appear in the spectra as pairs at fairly similar frequencies. It is also valuable to note that the ring-bridging oxygen atoms (Si-O-Si) contribute a vector (1) to the $\nu(\text{Si-O})$ representation, and the oxygen atoms external to the ring (Si-O-Ti and Si-O-Ba) contribute a different vector, (2); the order is that of the symmetry species in Table 1.

$$\begin{matrix} 1 & 1 & 2 & 0 & 0 & 0 \\ 1 & 1 & 2 & 1 & 1 & 2 \end{matrix} \quad (1)$$

$$\begin{matrix} 1 & 1 & 2 & 1 & 1 & 2 \end{matrix} \quad (2)$$

Stretching of Si-O-Si bonds is referred to as $\nu(\text{Si-O})_b$, and of the others as $\nu(\text{Si-O})_t$.

This necessarily lengthy discussion of the selection rules shows that a large amount can be predicted about the spectrum on the basis of logic-based arguments alone. Further refinement is possible on the basis of a normal co-ordinate analysis (n.c.a.) of the entire unit cell, but we consider that n.c.a. of a single ring would be little better than meaningless in view of the bonding in the crystal.

EXPERIMENTAL

A crystal of benitoite from San Benito County, California, was obtained on loan from the British Museum (Natural History), sample No. BM 19261463. Its morphology is shown in Figure 2, as are the axis sets used. The indicatrix

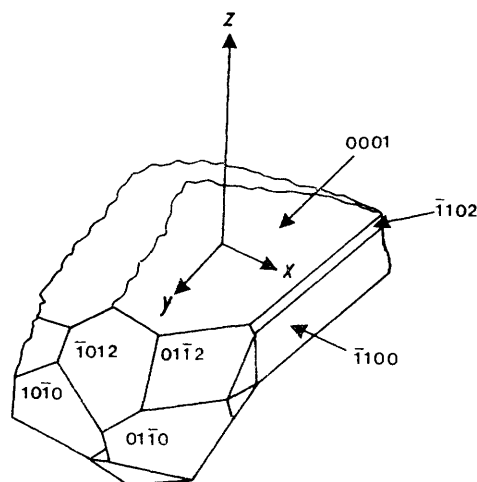


FIGURE 2 Morphology of the benitoite crystal used in this work

axes are (by definition) orthogonal and are labelled in accordance with Nye's convention.¹² Thus, x - and z - are identical with the crystallographic a - and c -axes, with y completing an orthogonal set and itself coincident with a crystallographic two-fold axis.

Raman spectra were obtained using a Coderg T800 (triple monochromator) instrument with 488.0 nm excitation from a Coherent Radiation Model 52A laser, and both 90 and 180° scattering geometry. Raman shifts are accurate to $\pm 0.5 \text{ cm}^{-1}$.

I.r. reflectance spectra at near normal incidence were obtained for the $(\bar{1}100)$ face, which is *ca.* $5 \times 2 \text{ mm}^2$. For the region 20–600 cm^{-1} a Beckman-RIIC FS-720 Fourier spectrometer was used with an RS7F reflectance module and a polyethylene-based wire-grid polariser. The region 200–5 000 cm^{-1} was covered using a Perkin-Elmer 225 spectrometer, and the reduced-focus reflectance accessory described elsewhere.¹³ The spectra were analysed by the Kramers-Krönig procedure; LO and TO frequencies were also estimated visually by taking the usual high- and low-frequency bounds of the reflectance regions.

Results and Assignment.—The observations are summarised in Tables 4–7 and Figures 3 and 4.

¹¹ R. Loudon, *Adv. in Physics*, 1964, **13**, 423.

¹² R. F. Nye, 'Physical Properties of Crystals,' Oxford, 1952.

¹³ D. M. Adams and M. M. Hargreave, *J.C.S. Dalton*, 1973, 1426.

TABLE 4
Raman frequencies (ν/cm^{-1}) and relative intensities for benitoite

	$x(\rho\sigma)y$			$x(\rho\sigma)z$			$x(\rho\sigma)\bar{x}$			$y(\rho\sigma)\bar{y}$			$z(\rho\sigma)\bar{z}$	
	xz	yx	zz	zy	yx	yy	zz	yy	yz	zz	zx	xx	yx	xx
78	16	4		9				13						
116		15			3									
125	7			4				8		5		4	6	
162	5	>100			37	35		6		3		28	46	
165								14			53			
181								3						
203	50			32				47		21				
222	82			51				89		60				
234	23			15				23		15				
268		66	70		16	44	18	32		55	>100		72	
348		52			15	40		21			85	10	49	
355		63			14	10						14	24	
362		>100			14			21			83			
372	81			54		14				60				
376		80			21			85						
396		14		8	4	4					4			
397	26							29		21		2	1	
467		40				7		5			23			
479		38			5							8	16	
504	5							6		5				
537			76			38	17	27	55		>100		61	
577			>100			>100	25	71	72		>100		100	
639			20				5		13					
750		5										2	3	
915		44			10	13						12	18	
928		>100			18	27		15			60			
929												20	30	
938	100			82		18		>100		100		14		
952	50	15		44	16	7		50		51		6		
1 022		12			3	2						4	6	
1 060			24			2	5	2	13		8		6	
1 096		9				1		2			9			
1 214		1												

A_1' Modes.—All the A_1' modes originate from silicate-ring vibrations since the Ti and Ba atoms do not contribute to this species. Five of the seven predicted modes were found.

In addition a weak and rather broad band appeared at 1 214 cm^{-1} in the $x(zz)y$ experiment only and is clearly of A_1' symmetry: together with the 1 060 cm^{-1} band it could account for the two expected $\nu(\text{Si-O})$ modes, although 1 214 cm^{-1} is much higher than any of the others. An alternative possibility is that the second $\nu(\text{Si-O})$ is at 929 cm^{-1} ; this is discussed below. Of the two $\nu(\text{Si-O})$ modes

TABLE 5

I.r. wavenumbers (cm^{-1}) of bands of A_2'' species for benitoite

Kramers-Krönig		Estimated	
LO	TO	LO	TO
84	76	81	72
379	352	376	307
460	400	436	391
1 088	932	1 100	924

TABLE 6

I.r. and Raman wavenumbers (cm^{-1}) of bands of E' species for benitoite

I.r.		I.r.		Raman ^a	
Kramers-Krönig		Estimated		Raman ^a	
TO	TO	LO	TO	LO	TO
1 088	1 014	1 100	1 018	1 096	1 022 ^b
970	920	970	926		929 ^c
				928	915 ^c
796	760	790	748		750 ^c
536	496	520	484		479 ^c
468	452	466	440	467	
408	384	397	378	396	376 ^c
365	356	363	356	362	355 ^c
		349			348 ^c
269	266	268	259	268	
168	162	165	158	165	162
138	124	133	116		116

^a Data from Table 4. ^b Brackets indicate pairs of coupled ring modes.

TABLE 7

Wavenumbers (cm^{-1}) of Raman bands of A_1' and E'' species for benitoite

A_1'	E''
(1 214)	952 ^c
1 060	938 ^c
929 ^b	504 ^c
639	397 ^c
577	372 ^c
537	234 ^c
268	222 ^c
	203 ^c
	181 ^c
	125 ^c
	78 ^c

^a Data from Table 4. ^b See text. ^c Brackets indicate pairs of coupled ring modes.

one is expected to have a strong (zz) component [since it is mainly $\nu(\text{Si-O})_t$] and this fits the 1 214 cm^{-1} band. The 639 cm^{-1} is only present in (zz) spectra and is hence most probably associated with $\delta(\text{SiO}_2)_t$ motion.

The lowest A_1' mode found is at 268 cm^{-1} and could be either a deformation or the sole 'rotatory' mode of this species, where that term implies a complex motion of the rings about the c -axis with accompanying deformation of

the Ti-O and Ba-O bonds. If it were the 'rotatory' mode it would have its greatest intensity in (xx) and (yy) spectra and be weak in (zz) but this is not the case. Accordingly we consider that the 'rotatory' mode is vanishingly weak.

other ring vibrations will likewise generate fairly closely spaced doublets. Part of the $\nu(\text{Si-O})$ separation of 14 cm^{-1} must be due to Fermi resonance, thereby indicating that the true correlation splitting is less than 10 cm^{-1} .

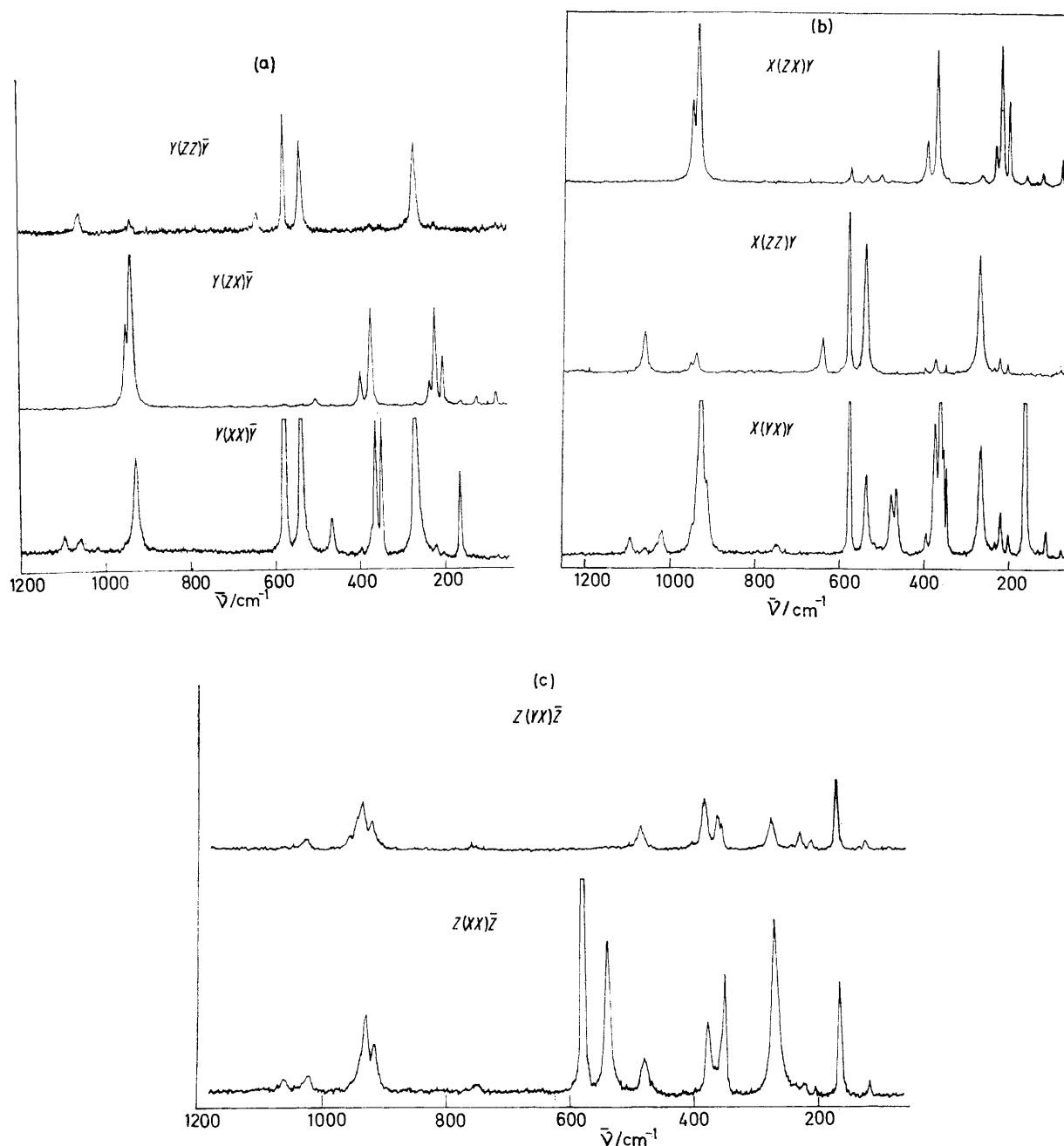


FIGURE 3 Single-crystal Raman spectra of benitoite. (a) $y(\rho\sigma)\bar{y}$ set. Spectral slit width 2 cm^{-1} , 175 mW 488.0 nm radiation at sample. (b) $x(\rho\sigma)y$ set. Spectral slit width 1 cm^{-1} , except for $x(zz)y$ which was 2 cm^{-1} ; 200 mW 488.0 nm radiation at sample, (c) $z(\rho\sigma)\bar{z}$ set. Spectral slit width 2 cm^{-1} , 175 mW 488.0 nm radiation at sample.

E'' Modes.—Eleven of the twelve predicted modes were found. Observation of the two $\nu(\text{Si-O})$ modes at 938 and 952 cm^{-1} is of significance for two reasons. They arise from coupling of a single e'' mode from each of two rings in the primitive cell. Their modest separation indicates that the correlation field is rather weak and further implies that all

Secondly, both of these $E'' \nu(\text{Si-O})$ modes are associated with the same set of oxygen atoms, *viz.* those on Wyckoff sites l and are Si-O-X bonded (X = Ti or Ba). Taken together with evidence from the other symmetry species this result shows that vibrations of Si-O-Si bonds are at *higher* frequencies than those of Si-O-X.

Coupling of the $4e''$ modes from each of two rings is expected to yield four *pairs* of bands in the E'' spectrum; one has been located ($938/952\text{ cm}^{-1}$), leaving three others: the rather obvious choice is $397, 372$ (25); $234, 222$ (12); and $203, 181$ (22) cm^{-1} , where the splittings are given in parentheses, and also contain a Fermi resonance contribution. This leaves 125 and 78 cm^{-1} as lattice modes associated with ring and Ba^{2+} motion, although they must interact strongly with the lower 'internal' modes. The band at 504 cm^{-1} is conspicuous in having no close-lying component: two explanations are envisaged. (i) There really is a missing band nearby: this implies that one of the above doublets is fortuitous, probably the lowest one. (ii) Since, as we have argued above, the Ti-O bonds are expected to be as strong as in rutile (which has optically-active phonons as high as 825 cm^{-1}), the 504 cm^{-1} band is the single $E''\nu(\text{Ti-O})$ stretch expected on the basis of Table IA. We incline to the latter view.

A_2'' Modes.—The i.r. reflectance spectra obtained with the electric vector parallel to the c -axis clearly showed four of

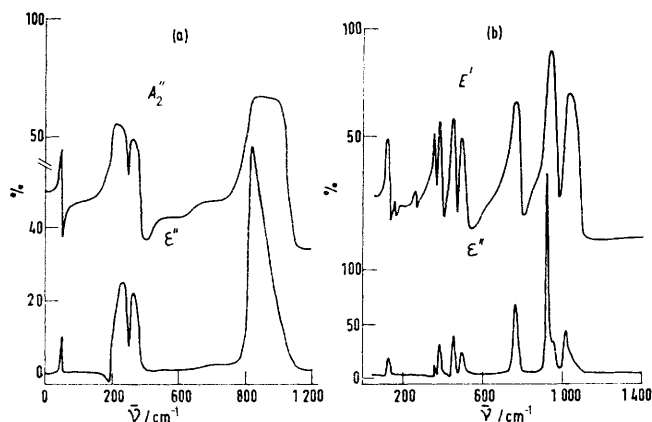


FIGURE 4 I.R. reflectance spectra of benitoite. (a) A_2'' species, (b) E' species. In each case the upper curve represents the observed percentage reflectance, and the lower one the function ϵ'' derived by Kramers-Krönig analysis. [$\epsilon^* = \epsilon' - i\epsilon''$ and $\epsilon^* = (n^*)^2$]

the expected six modes, including the sole $\nu(\text{Si-O})_t$, which, for the reasons outlined under E'' , is associated with the Si-O-X bonds. One of the A_2'' modes originates from the rings as a mode which would be inactive, a_1'' and basically $\rho_r(\text{SiO}_2)$ if the ring had true D_{3h} symmetry and not C_{3h} (due to an alternation of bond lengths of 1.458 and 1.646 \AA): it may be very weak and hence not observed in the reflectance spectra. The bands at 391 and 307 cm^{-1} are probably due to modes involving ring out-of-plane and $\rho_r(\text{SiO}_2)$ coordinates.

By analogy with the E'' results, it is expected that the inactive A_1'' crystal modes will have values $\pm 25\text{ cm}^{-1}$ from the above A_2'' modes.

E' Modes.—Each ring has $6e'$ internal modes [two of them being $\nu(\text{Si-O})$ in type] which, when coupled in the crystal, will yield $12E'$ modes in pairs. In addition there are three translatory modes involving motion of Ti, Ba, and the rings relative to each other, and having the descriptions of Table IA or B.

The i.r. reflectance spectra obtained with the electric vector normal to the c -axis showed ten of the fifteen predicted bands of E' symmetry including at least two of the four $\nu(\text{Si-O})$ modes (see Figure 4).

The particular interest of this crystal is that, since it is non-centrosymmetric, the Raman spectra provide an independent means of observing both TO and LO modes (see Table 3). It is clear from the results that the $E'(\text{TO})$ Raman spectra do not contain all the bands expected on the basis of the i.r. spectrum (e.g. 259 and 440 cm^{-1} are missing), and the $E'(\text{LO})$ spectrum shows only seven bands of observable intensity of which only three ($165, 396,$ and 1096 cm^{-1}) obviously form pairs with appropriate bands from the $E'(\text{TO})$ spectrum. Nevertheless, with two apparent exceptions discussed below, there is excellent agreement between the LO and TO frequencies determined independently from Raman and i.r. experiments, as can be seen from Table 6. Thus, although neither type of spectrum contains the full information, combining evidence from them allows identification of twelve of the fifteen bands predicted. We consider each region in turn.

The 116 cm^{-1} $E'(\text{TO})$ band is strong in i.r. reflectance but weak in the Raman spectra, in which it shows no sign of a TO component. A strong and clearly separated Raman TO-LO pair are at $162, 165\text{ cm}^{-1}$ corresponding to a weak i.r. band; but the i.r. TO mode at 259 cm^{-1} has no Raman counterpart.

The Raman spectra clearly show the presence of three modes in the $340\text{--}400\text{ cm}^{-1}$ interval. Three $E'(\text{LO})$ bands are at $349, 362,$ and 396 cm^{-1} ; the two highest correspond to i.r.-determined LO frequencies but that at 349 cm^{-1} does not, although it is coincident (within experimental error) with an i.r. and Raman-active TO frequency. We conclude that there is a near accidental-degeneracy at $348/349$ and $355/362\text{ cm}^{-1}$ and attribute this to weak correlation coupling of e' modes.

Two strong i.r. bands with TO components at 440 and 484 cm^{-1} have Raman counterparts but for the higher band the LO is missing and for the lower one, the TO. This again shows the complementary nature of the two sets of spectra, and indicates the ease with which a mis-assignment of Raman data alone could have been made. The intense 748 cm^{-1} i.r. TO mode has an extremely weak Raman equivalent; this band could well be associated with $\nu(\text{Ti-O})$ motion.

I.r. reflectance data above 900 cm^{-1} are consistent with the presence of two $\nu(\text{Si-O})$ modes with TO frequencies at 915 and 1018 cm^{-1} . However, the observation of a prominent Raman mode at 929 cm^{-1} in the $y(xx)y$ spectrum raised the possibility that there may be a further mode in near-coincidence. Raman emission in the region $910\text{--}960\text{ cm}^{-1}$ is fairly complex. The simplest to interpret is the $z(yx)z$ spectrum which should yield $E'(\text{TO})$ only: it has weak residuals of E'' origin but also clearly shows genuine E' emission at 915 and 929 cm^{-1} , also present in $z(yy)z$ and $z(xx)z$ which yield $A_1' + E'(\text{TO})$ species together. Emission close to 929 cm^{-1} is therefore compatible with the presence of either an E' fundamental or E' and A_1' fundamentals in accidental coincidence. Its strength inclines us to the latter view.

Summarising our E' assignment: three of the four $\nu(\text{Si-O})$ modes have been located. The rest of the spectrum must contain four *pairs* of internal modes and three translatory modes; two of these translatory modes (those due to Ba^{2+} and the rings) will be not higher than 200 cm^{-1} and are most probably to be identified with the 162 and 116 cm^{-1} bands. The third 'translatory' mode is associated with titanium and is more properly regarded as $\nu(\text{Ti-O})$; it is probably at 750 cm^{-1} . By elimination we regard the

following as pairs of internal modes generated by coupling of two sets of $4e'$: 479, 440(39); two overlapping pairs at 376, 355, and 348 cm^{-1} ; and a final pair of which only the 259 cm^{-1} component was found.

Comparison with Beryl.—We recently reported a full assignment to symmetry species of the spectra of beryl,⁶ but only the $\nu(\text{Si-O})$ region was discussed in any detail. In the light of our study of benitoite, further comment on beryl is now valid: the very complicated spectra of both materials can be understood on the basis of a single model, which we expect will be applicable generally in similar circumstances.

300—800 cm^{-1} region, and again in A_{2u} . However, in E_{1u} and E_{2g} spectra the appearance of several conspicuously single bands lends support to our general method of assignment. In the E_{2g} spectrum all the low-frequency bands must be due to ring internal modes as the only 'translatory' modes allowed are really $\nu(\text{Al-O})$ and $\nu(\text{Be-O})$ and are at higher frequency. Two ring rotatory modes are expected in E_{1g} and may or may not have been observed as two modes are missing from this spectrum. However, there must be considerable interaction between them and the lower ring modes.

TABLE 8

Wavenumbers (cm^{-1}) and assignment for beryl ^a

A_{1g}	$\nu(\text{Si-O})$	1 125, 1 068						
	Others	686, 626, 396, 324, 214						
A_{2u}	$\nu(\text{Si-O})$	924						
	Others	734, 532, 419, 361, 201						
E_{1g}	1 012 } ^c	$\nu(\text{Si-O})$	E_{2g}	1 243 } 1 225 } 1 005 } 914 } 772 } 685 } 583 } 565 } 444 } 424 } 397 } 318 } 291 } 187 } 146 }	$\nu(\text{Si-O})$	E_{1u}	1 200 } 1 014 } 958 } 796 } 682 } 656 }	$\nu(\text{Si-O})$
	918 } 770 } 683 } 529 } 450 } 383 }	$\nu(\text{Be-O})$ $+\nu(\text{Al-O})$			$\nu(\text{Be-O})$		$\nu(\text{Be-O})$	
	297 } 254 } 188 } 145 }				$\nu(\text{Al-O})$		$\nu(\text{Al-O})$	
	b }							

^a Data from ref. 6. ^b Presumed position of unobserved band. ^c Brackets indicate pairs of coupled ring modes.

The spectra may be regarded as constructed from pairs of vibrations, one from each of the two rings per unit cell, which typically have separations of up to 50 cm^{-1} [apart from $\nu(\text{Si-O})$]. These are interspersed with modes due to counterion-silicate motion, which may be very high in frequency if that bonding is strongly directional. Thus, for beryl, we indicate in Table 8 a scheme of pairing of observed modes and assignment to counterion-silicate oxygen motion. These are only approximate descriptions but they could be improved only by a n.c.a. of the entire unit cell. There is good internal evidence for interaction between ring and $\nu(\text{Al-O})$ and $\nu(\text{Be-O})$ modes in the E_{1g} spectrum in the

Conclusions.—We believe that we have established the assignment for most of the vibrational spectrum of benitoite, but several points remain to be settled conclusively. Further work is dependent upon acquisition of a high quality specimen with better face development, or one which can be cut and polished. A better test of the E' assignment, in particular, will then be possible, and i.r. reflectance at oblique incidence worthwhile.

We thank the British Museum (Natural History) for loan of the benitoite crystal, and the S.R.C. for a grant to I. R. G.

[5/1023 Received, 28th May, 1975]